E12-12-006 Jeopardy Update to PAC50

Near-Threshold Electroproduction of J/ψ at 11 GeV

S. J. Joosten,[1] Z.-E. Meziani (contact),[1,*] X. Qian,[2] N. Sparveris,[3] and Z. Zhao[4]
(The SoLID-J/ψ Collaboration [b])

[1] *Argonne National Laboratory, Lemont, IL*
[2] *California Institute of Technology, Pasadena, CA*
[3] *Temple University, Philadelphia, PA*
[4] *Duke University and Triangle Universities Nuclear Laboratory, Durham, NC*

(Dated: May 15, 2022)

The experimental landscape for near-threshold J/ψ production has dramatically changed since the original proposal of the SoLID-J/ψ experiment. The first results on the near-threshold cross section from GlueX trend significantly higher [1] than what we originally extrapolated from the Cornell [2] and SLAC [3] data. This higher cross section dramatically increases the science reach of SoLID-J/ψ. The photoproduction channel will have an unprecedented reach to precisely measure the two-dimensional cross section over the entire phase space with photon energies above 8.4 GeV, including the hard-to-measure high-t region. Complementary to the photoproduction channel, the electroproduction channel will yield the full t-dependence at the threshold, with virtualities of about 1 GeV^2. Furthermore, comparing the photoproduction to electroproduction results will provide a modest but important lever arm in Q^2 in the threshold region.

I. INTRODUCTION

Since the 2012 approval of the original proposal for the SoLID-J/ψ experiment, the scientific motivation and community interest to measure J/ψ production have strengthened due to a few high-profile events. First, the announcement of the LHCb charmed pentaquarks in 2015 [4] inspired a large body of work, including suggestions that the particle can be accessed in photoproduction of J/ψ at Jefferson Lab due to energy reach and luminosity. This spurred several experimental efforts in Hall B (CLAS12), Hall C (J/ψ-007), and in Hall D (GlueX). In parallel to these developments, the NAS report on the EIC [5] (published in 2017-2018) recognized the question on the origin of the proton mass to be of fundamental importance. This development positions the SoLID-J/ψ program to be complementary to one of the cornerstone topics of the EIC.

In light of the first near-threshold results from the GlueX experiment [1], and the new results from the Hall C J/ψ-007 experiment, the theoretical activity to interpret these near-threshold J/ψ measurements has caught the imagination of the wider community. Recent theoretical developments [6–22] have touched on topics such as the origin of the proton mass, observables related to the trace anomaly of the energy momentum tensor, and the extraction of gluonic gravitational form factors and gluonic radii from experimental data. The sustained community interest, supported by a series of workshops since 2016, will continue in the future due to the strong synergy with the EIC scientific program. A fourth dedicated workshop on these topics will be held in June 2022 at the INT.

The comprehensive J/ψ production program at Jefferson Lab has already produced interesting results that have transformed our knowledge of this process. GlueX measured a near-threshold cross section for J/ψ production [1] significantly above the trend from the old Cornell [2] and SLAC [3] results. This was tentatively confirmed with the new results from Hall C. This enhanced cross section strengthens the SoLID J/ψ program, as it allows us to measure the differential J/ψ production cross section with good precision up to high values of t, a region that cannot be accessed by any other experiment. We update some of the key projections for SoLID-J/ψ based on these new developments.

---

[b] see the full collaboration list at https://solid.jlab.org/collaboration/jpsi.html
[*] zmeziani@anl.gov

II. PROGRESS ON THE SOLID APPARATUS

Since the first PAC approvals in 2010 of five SoLID experiments with high rating, the collaboration has developed a Pre-CDR [23] with details on the SoLID apparatus as well as a cost estimate. In 2015, the SoLID apparatus and its approved experimental program received a strong endorsement from the Nuclear Physics Long Range Plan. In September of 2019, the Pre-CDR successfully passed the second of two Jefferson Lab Director's Reviews. The latter review covered a detailed cost estimate and detailed analysis that found all critical items to be low risk. The Pre-CDR was the basis of the SoLID MIE submitted to the DOE in February of 2020. In 2020, the DOE funded a Pre-R&D plan, which demonstrated that there are no show-stoppers in the SoLID design. In March of 2021, the DOE performed a Science Review of the SoLID experimental program. We give a brief overview of the features of the SoLID apparatus and pre-R&D progress below.

In the Pre-CDR, we have demonstrate that the apparatus can achieve the following goals:

1. High luminosity (10^{37} cm^{-2}s^{-1} for SIDIS and J/ψ, 10^{39} cm^{-2}s^{-1} for PVDIS with baffles)
2. Large acceptance: 2π in azimuthal angle ϕ; In polar angle θ: $8^\circ - 24^\circ$ for SIDIS and J/ψ, $22^\circ - 35^\circ$ for PVDIS: Momentum range: $1 - 7$ GeV/c
3. High rates (trigger rate limit 100 KHz for SIDIS and J/ψ, 600 KHz of the 30 sectors for PVDIS)
4. High background tolerance ($\sim$1 GHz, dominated by low energy photons/electrons)
5. High radiation environment tolerance (10^{2-3} krad)
6. Moderate resolutions ($1 - 2\%$ in momentum, $1 - 2$ mrad in θ, 6 mrad in ϕ)
7. Good electron PID; moderate pion PID (SIDIS), and demanding Kaon PID (SIDIS-Kaon, enhanced configuration)
8. High precision with low systematic effects

The SoLID apparatus in its J/ψ configuration with LH_2 target is shown in Fig. 1. Since the original proposal, we have optimized the experiment to use the SoLID SIDIS setup without any detector changes. The only difference with the SIDIS setup is the LH_2 target position, which is placed further downstream compared to the SIDIS ^{3}He target to optimize the acceptance. Furthermore, we optimized the trigger design based around the two decay leptons only, allowing both electroproduction and photoproduction data to be collected simultaneously, while the trigger rate remains below the SoLID SIDIS setup limit of 100kHz.

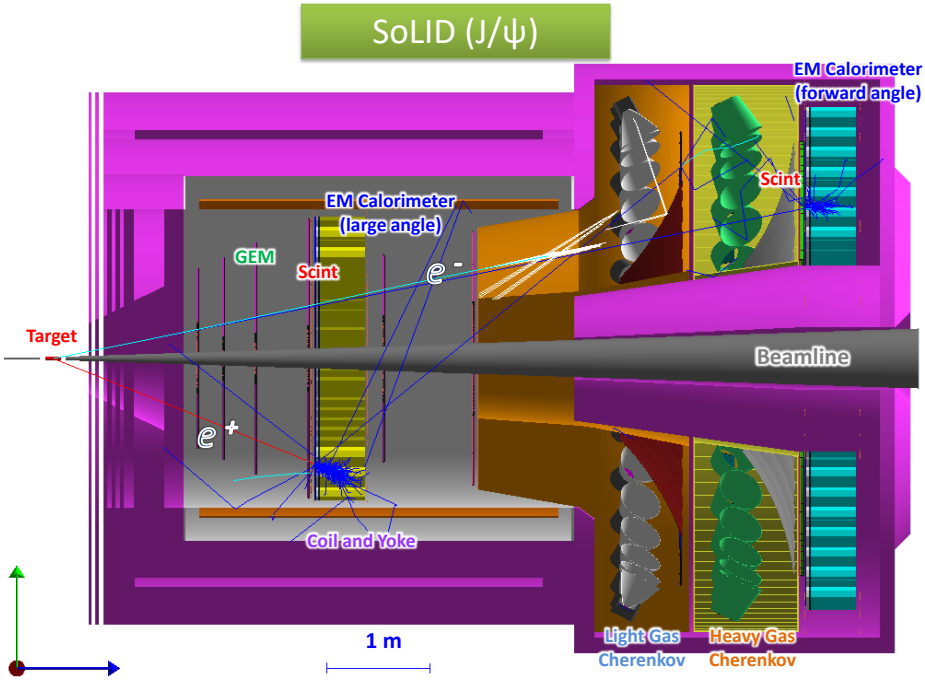

FIG. 1: SoLID-J/ψ Setup with LH_2 target

Since the SoLID experiments were approved, the CLEO magnet, located at Cornell University, was chosen. Jefferson Lab requested the magnet in 2012 and it was moved to Jefferson Lab in 2016, along with most of the required return iron. Jefferson Lab is currently performing minor refurbishment of the magnet and preparing for a cold test to establish the magnet's operational condition. The cold test is scheduled to be completed before the end of 2022.

Significant progress has been made in all subsystems, and many components have been tested and shown to meet specifications. The UVa group has built large GEM chambers with the required sizes for SoLID. They successfully manufactured and operated GEM detectors for the PRad experiment and SBS experiment. During our recent execution of the Pre-R&D plan, we tested the new VMM3 GEM readout chips, which we plan to use instead of the obsolete APV25 chips listed in the original proposals. We have demonstrated that the VMM3 chips operated in a mode with a 25 ns shaping time can handle the high rates required for SoLID.

The Scintillator Pad Detector (SPD) has undergone extensive cosmic testing to benchmark its timing and position resolution. The fine-mesh PMT which will be placed on the edge of the solenoid field to read out the large-angle SPDs was tested under a magnetic field up to 1.9 T, and its gain and timing resolution were characterized [24].

A prototype Cherenkov was beam-tested in Hall C in 2020, both at low rates and also at high rates equal to those expected in the SoLID spectrometer. In both the low and high rate configurations, clean signals could be identified and the overall electronics performed very well.

The ECal prototype modules were successfully tested at the Fermilab Test Beam Facility in January of 2021. The data showed that the energy resolution of the 3-module setup reached the SoLID requirement of $\delta E/E = \sqrt{10\%}/\sqrt{E}$ and the position resolution exceeded the required 1 cm specification.

The SoLID DAQ system is based on Jefferson Lab 12 GeV FADC base pipelined electronics, which now have been successfully used in Halls B and D. Special features of the Jefferson Lab FADC required for SoLID, which were built into the Jefferson Lab design but never used in previous applications, have now been successfully tested for all systems as part of the SoLID Pre-R&D plan.

Currently, a beam test of a full set of SoLID detector prototypes – GEM, LGC, ECal, DAQ and associated electronics – is in preparation. The goal of the test is to fully characterize the functionality of the detector system under a high-rate, high-radiation environment that is similar to the SoLID operational conditions.

The SoLID simulation software, based on GEMC/GEANT4, is a single package that is used to model all approved experiments and run-group experiments. It is being used to optimize the design and evaluate the impact of the results from the past and ongoing tests. A Kalman Filter based track finding and fitting algorithm was developed and tested with fully digitized GEM simulation data. Tracking resolutions with good tracking efficiency were obtained with background taken into account. We are actively working on assembling simulation, reconstruction, and analysis into a unified software toolkit.

III. SIMULATION

We based our updated projections around a new 2+3 gluon fit to the 2019 GlueX results on near-threshold J/ψ photoproduction. To conservatively account for the 27% scale uncertainty on the GlueX results, we lowered the points by this value prior to fitting. The fit is shown in Fig. 4 as a solid curve. We assumed an exponential t-dependence for all projections, as it falls off quicker than a typical dipole shape. We used the lAger Monte-Carlo generator [25, 26], which includes radiative effects on the J/ψ decay, to generate two Monte-Carlo samples for 50 days of running at the nominal luminosity. The first Monte-Carlo sample corresponds to electroproduction, while the second sample corresponds to photoproduction due to bremsstrahlung generated in the extended target cell. Both samples are added together before being passed through a fast simulation of the SoLID detector, based around acceptance and resolution maps that were obtained from the full SoLID simulation and reconstruction software.

IV. NEW PROJECTIONS: PRODUCTION WITH QUASI-REAL PHOTONS

The photoproduction channel receives approximately equal contributions from quasi-real electroproduction events and direct photoproduction events due to bremsstrahlung in the extended target. The photoproduction channel maximizes the statistical impact the SoLID-J/ψ experiment can achieve. We measure these events by requiring a coincidence between the J/ψ decay electron-positron pair and the recoil proton. As in the original proposal, the decay pair can be identified with the light-gas Cherenkov and electromagnetic calorimeter in the forward direction, and with the wide-angle electromagnetic calorimeter at larger angles. The recoil proton kinematics are shown on Fig. 2 (left). The recoil proton, which is relatively slow, can be identified through time-of-flight (TOF) at larger angles through the SPDs, which have a 150 ps time resolution (travel distance about 2.6 m). At forward angles, the TOF MRPC,

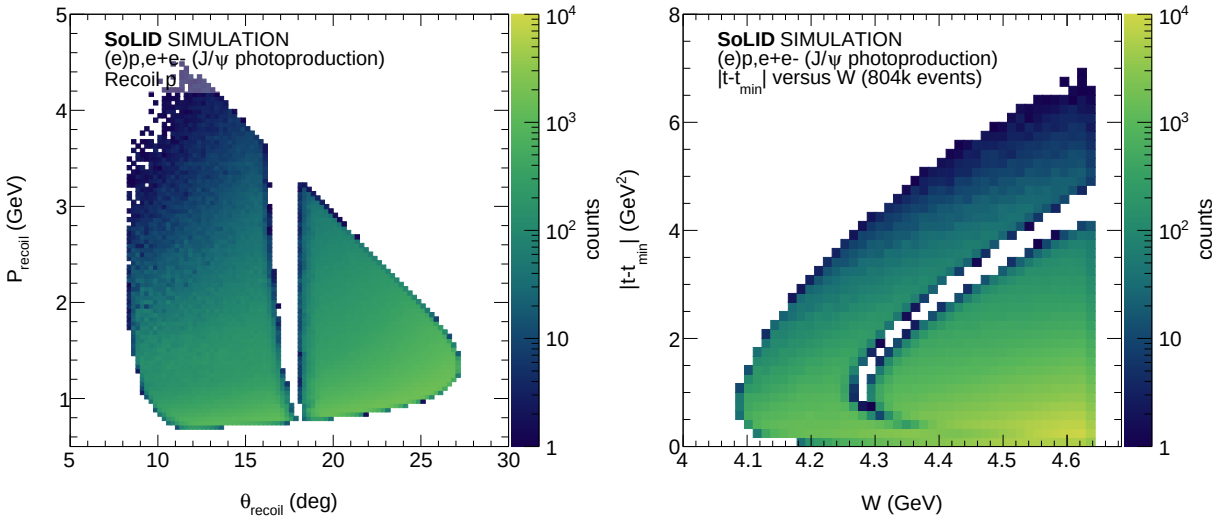

FIG. 2: Left: Recoil momentum as a function of polar angle θ. Right: Phase space coverage in the Mandelstam variable $|t - t_{\rm min}|$ versus the invariant mass of the final state W. The very high statistics with the photoproduction channel allow for a precise measurement of the t-dependence of the cross section, even at high t. Both figures correspond to the nominal luminosity for the SoLID-J/ψ experiment.

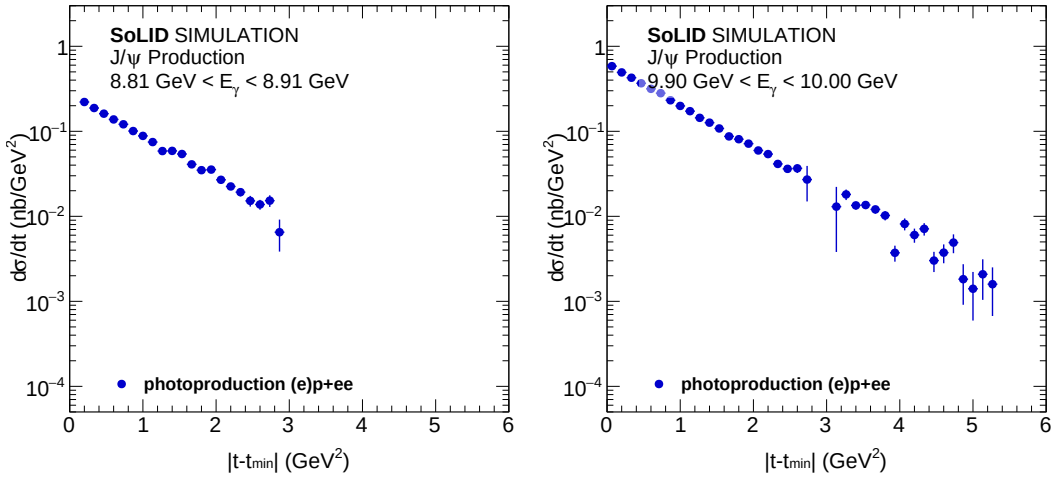

FIG. 3: The projected differential cross section for a photoproduction bin at low (left figure) and high (right figure) photon energy from Figure 4, assuming the nominal luminosity for SoLID-J/ψ. Photoproduction will hold the key to measure the shape of the t-dependence in high precision over the entire phase space.

with 30 ps time resolution, is more than sufficient to identify the protons (travel distance about 8 m). In the absence of the MRPCs, the forward SPDs could also be used to identify the protons.

The phase space coverage in the Mandelstam variable $|t - t_{\rm min}|$ versus the invariant mass of the final state W for the photoproduction channel is shown in Fig. 2 (right). The projected statistics and acceptance are sufficient to make a precise measurement of the differential cross section up to very large values of t. The photoproduction channel cannot fully reach the J/ψ threshold due to limited acceptance for these events. Within the SoLID configuration, this region is accessible through production with virtual photons (see the next section). The small gap in the phase space coverage at intermediate t is caused by the gap between the forward and wide-angle detector systems.

The projected one-dimensional cross section results for photoproduction are shown as the solid blue disks on Fig. 4, compared with the projected electroproduction results, and the existing world data from GlueX and Cornell. The statistical uncertainties are exceedingly small on this figure. The power of this high-luminosity, high-acceptance measurement is illustrated in Fig. 3. The panels correspond each to a single point in Fig. 4. The enormous statistical

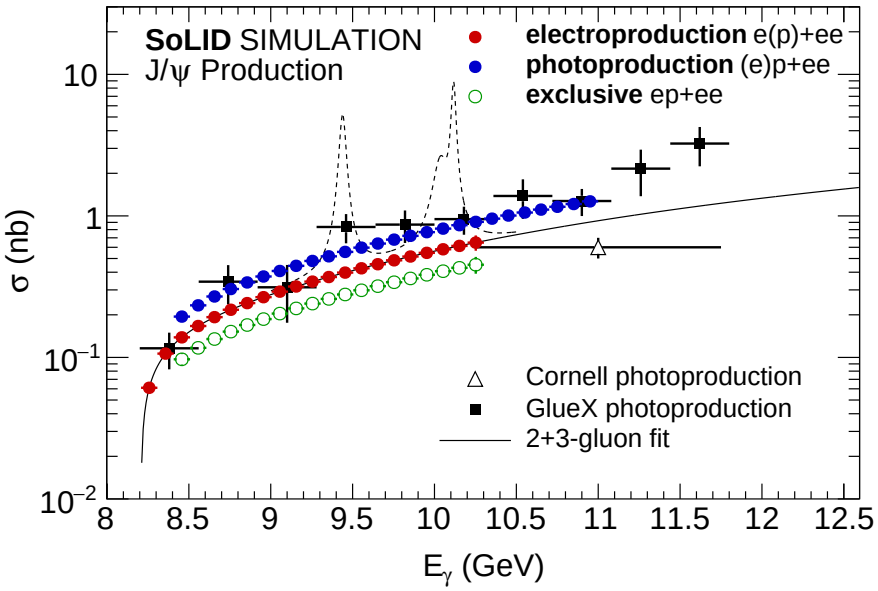

FIG. 4: Projected one-dimensional cross section coverage for SoLID-J/ψ, compared to the available world data (black markers). The SoLID projections are based off a 2+3 gluon fit to the GlueX data, lowered by the scale uncertainty (solid curve). The figures shows quasi-real production (blue disks), production with virtual photons (red disks), and fully exclusive electroproduction (green open circles). The different colored points are vertically offset for clarity. The kinematics for electroproduction allow for a precise measurement all the way down to the threshold. Also indicated are the location of the LHCb charmed pentaquarks (dashed curves). Each of the SoLID projected points has enough statistics and acceptance to allow for a precise measurement of the t-dependence.

power of the SoLID-J/ψ experiment enables a precise measurement of t-dependence at very large values of t. Measuring the entire t-dependence up to very high t is crucial to constrain model uncertainties when linking these results with the gluonic structure of the proton. This high-t measurement is not possible with any other current or future experiment.

V. NEW PROJECTIONS: PRODUCTION WITH VIRTUAL PHOTONS

Exclusive J/ψ electroproduction was the cornerstone of the original proposal. It provides a two-dimensional measurement of the cross section down to the threshold, while providing a modest lever arm in Q^2. To measure the electroproduction events, we measure the scattered electron in coincidence with the J/ψ decay electron-positron pair. For a subset of events, we also detect the recoil proton for a full exclusive measurement, a redundant measurement important to understanding the physics and detector backgrounds, necessary to precisely determine the absolute cross section. The scattered electron is detected in the forward spectrometer, using the light-gas Cherenkov and electromagnetic calorimeter for particle identification. The particle momentum as a function of scattering angle is shown in Fig. 5, where the left figure shows the scattered electron and the right figure the decay electron (or positron).

The phase space in $|t - t_{\rm min}|$ versus W for electroproduction is shown in Fig. 6 (left). While the overall statistics are lower than for quasi-real production, the kinematics for production with a virtual photon lead to a good acceptance for events at the threshold. Furthermore, the electroproduction channel has a very good reach in t at lower values of W, exceeding the reach for the photoproduction channel up to W of about 4.3 GeV. In this respect, the virtual J/ψ production measurement is truly complementary to the quasi-real channel: quasi-real has superior statistics and t-reach at higher W, while virtual production has superior reach in the region very close to the threshold. The relation between the photon virtuality Q^2 and W are shown in Fig. 6 (right). The average Q^2 at threshold is about 1 GeV^2, dropping as a function of W. Combining the electroproduction results with the photoproduction results yields a modest but important lever arm in Q^2.

The one-dimensional projections for virtual photon production are shown on Fig. 4 as red disks and the fully-exclusive projections are shown as green open circles. The lower-energy focus for this measurement is apparent from the figure: there is reach towards the threshold, while the high-energy acceptance stops at photon energies of about 10.3 GeV for an 11 GeV incident beam. Similar as for the photoproduction case, each of the markers has

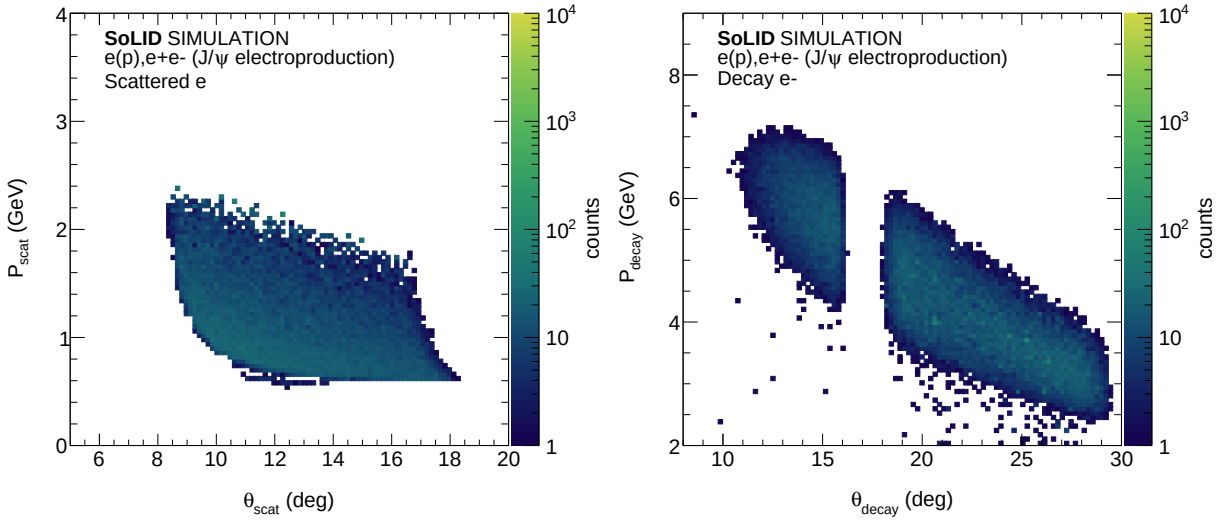

FIG. 5: Particle momentum as a function of polar angle θ for the scattered electron and decay leptons for exclusive electroproduction of J/ψ near threshold.

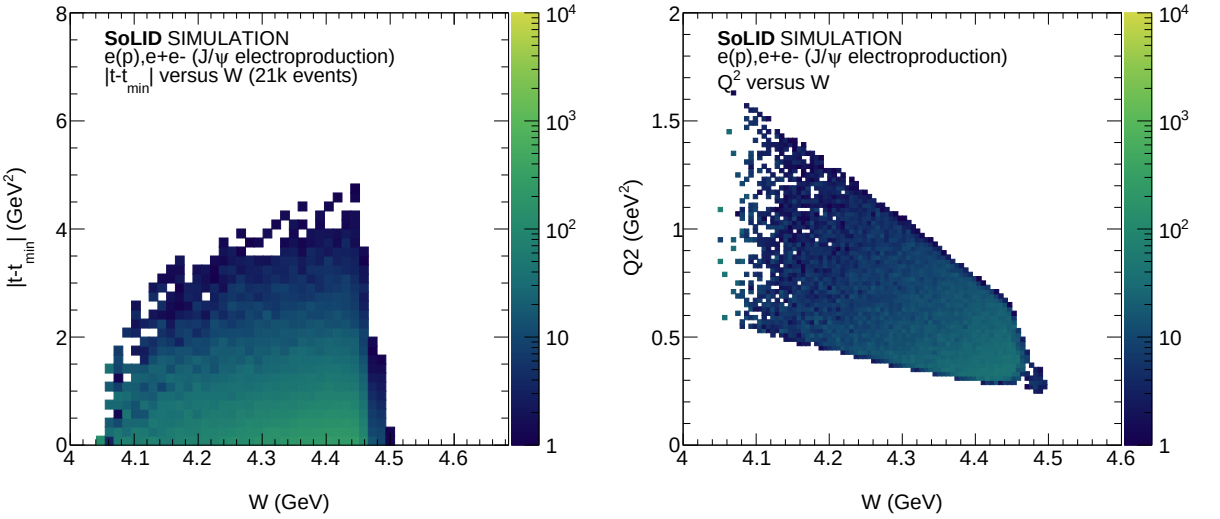

FIG. 6: Phase space coverage for exclusive electroproduction of J/ψ near threshold at SoLID. Left: Mandelstam variable $|t - t_{\rm min}|$ versus the invariant mass of the final state W. The improved kinematics with electroproduction allow us to measure the 2D cross section all the way to the threshold. Right: Photon virtuality Q^2 versus W. At threshold, the average value of Q^2 is about 1 GeV^2. Both figures correspond to the nominal luminosity for the SoLID-J/ψ experiment.

a corresponding measurement of the t-profile of the cross section, illustrated in Fig. 7 for two such bins. In both examples, the t-range extends well into the high-t region.

VI. COMPARISON WITH OTHER EXISTING AND FUTURE EXPERIMENTS

As mentioned in the introduction, the increased profile of the physics topics that can be studied through near-threshold quarkonium production has spurred many experimental efforts at Jefferson Lab and is an important component of the EIC scientific program. Below is an overview of the current and future near-threshold J/ψ program at Jefferson Lab and the feasibility for a near-threshold quarkonium program at the EIC, compared to the SoLID-J/ψ program:

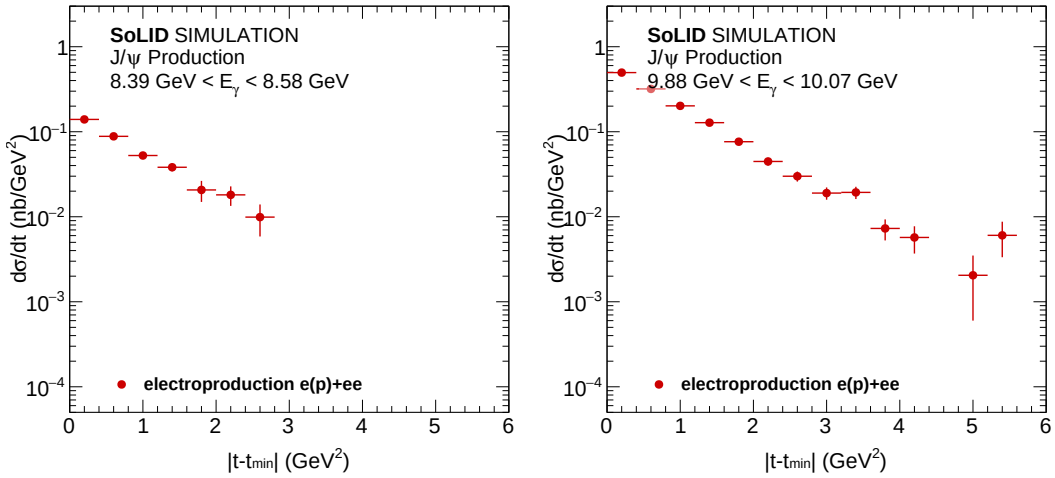

FIG. 7: The projected differential cross section for an electroproduction bin at low (left figure) and high (right figure) photon energy from Figure 4, assuming the nominal luminosity for SoLID-J/ψ.

GlueX: The GlueX results from 2019 [1] showed that the photoproduction cross section near threshold is significantly larger than what would be extrapolated by low energy measurements from SLAC and Cornell. The publication included about 500 measured J/ψ events. Based on the existing results, we expect a total dataset from GlueX, including run I and run II, of about 10,000 J/ψ events. With this luminosity, GlueX will not have the reach to measure the cross section at high $|t - t_{\rm min}| > 2$ GeV^2. Finally, GlueX uses a real photon beam, and cannot access the electroproduction channel.

Hall C: The Hall C J/ψ experiment was designed to search for the LHCb charmed pentaquark [27]. It measured about 4000 J/ψ in total, spread over 4 kinematic regions. Between these regions, the Hall C results are the first 2D cross section measurement in the threshold region. The Hall C results do reach higher values of t compared to GlueX (up to about 4.5 GeV^2), but only at higher photon energies, and with low statistical precision. Improving on this is limited by the spectrometer acceptance, as it makes both going closer to the threshold and going to higher t difficult. Hence, a meaningful increase on the statistics to be competitive with SoLID at low photon energies or high t, which entails extended running with a radiator, is impractical.

CLAS12: The CLAS12 collaboration is currently analyzing it's first J/ψ results. Assuming the proposed luminosity upgrade for CLAS12, we project a total of about 14,000 measured photoproduction events (measuring the e^+e^-p final state) and 1,000 measured electroproduction events. The photoproduction channel will be of similar statistical significance as GlueX, while the electroproduction channel should be sufficient for a first (low-precision) measurement near threshold.

EIC: While the EIC in principle creates J/ψ at threshold, these events are very hard to reconstruct due to limited resolution for events at very low $y = P\cdot q/P\cdot k$ [28]. This limits the threshold quarkonium production program at EIC to heavier particles, where the threshold events can be more precisely measured. Foremost in this program is the measurement of Υ production near threshold. This measurement will be complementary to the SoLID J/ψ measurement, trading statistical precision (the Υ cross section is much lower than the J/ψ cross section) for lower theoretical uncertainties (the Υ is more point-like due to its heavier mass).

TABLE I: Overview of the current and projected future event counts for the J/ψ program from Jefferson Lab, compared to SoLID. The CLAS12 projection assumes a modest luminosity upgrade to 2×10^{35}cm^{-2}s^{-1}.

Experiment	GlueX (Hall D)	J/ψ-007 (Hall C)	CLAS12 (Hall B)	SoLID (Hall A)
J/ψ photoprod.	469 (published)	2k (e^+e^-)	14k	804k
	10k (phase I+II)	4k ($e^+e^- + \mu^+\mu^-$)		
J/ψ electroprod.	N/A	N/A	1k	21k

A comparison of the projected statistics with the rest of the Jefferson Lab J/ψ program can be found in Tab. I. SoLID will be required to measure the differential J/ψ production cross section with reasonable precision over the

full phase space. Reaching higher values of t ($|t - t_{\min}| > 2$ GeV^2) near threshold will not be possible with any of the other existing and projected experiments. Furthermore, only SoLID will have the statistics to conduct a high-precision measurement of the electroproduction cross section for J/ψ near threshold.

VII. UPDATE ON RUN GROUP EXPERIMENT OF TIMELIKE COMPTON SCATTERING: E12-12-006A

(Spokesperson: Marie Boer, Pawel Nadel-Turonski, Jixie Zhang, Zhiwen Zhao (contact))

The run group experiment "Timelike Compton Scattering on the proton in e^+e^- pair production with SoLID at 11 GeV" E12-12-006A [29] was approved in 2015 by the SoLID Collaboration and PAC 43. It is to study Timelike Compton Scattering (TCS) reaction via exclusive e^+e^- production, using the SoLID detector with an 11 GeV polarized electron beam and a 15 cm LH_2 target. As it detects similar final state particles like the SoLID J/ψ experiment E12-12-006, the two measurements would benefit each other on the normalization and systematic studies.

The Generalized Parton Distribution Functions (GPDs) describe the nucleon parton distributions in the combined one longitudinal-momentum dimension and two transverse-space dimensions. The Deeply Virtual Compton Scattering (DVCS) process was studied by many experiments to access GPDs. In addition to DVCS using a real spacelike photon, one can also access the same GPDs through TCS using a virtual timelike photon. A comparison with DVCS can test the universality of GPDs, while a combined fit to both DVCS and TCS observables can reduce the uncertainty on the measured Compton Form Factors (CFFs), making the two processes complementary. TCS process in Eq. 1 which is the photoproduction of a virtual timelike photon ($Q'^2 > 0$) on a nucleon, where the final-state virtual photon immediately decays into a lepton pair, as shown in the left panel of Fig. 8 [30].

$$\gamma + p \to \gamma^* + p' \to e^- + e^+ + p' \tag{1}$$

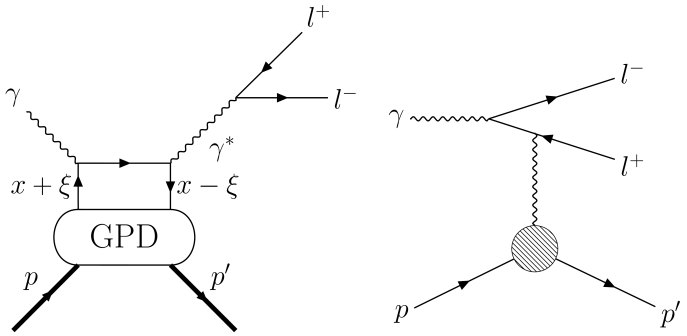

FIG. 8: Left: handbag diagram of the TCS process. Right: diagram of the BH process.

TCS is not the only physical process that can be observed in the exclusive photoproduction of lepton pairs, many resonance states decay into lepton pairs as well. In the resonance free region, the dominant background process with the same final state is the purely electromagnetic Bethe-Heitler (BH) reaction shown in the right panel of Fig. 8. Like DVCS, the TCS and BH amplitudes interfere. Even though the BH cross section is significantly larger than the TCS cross section, we can take advantage of this interference to study TCS.

Since the SoLID TCS experiment approval in 2015, there are more theoretical progress made in TCS studies [31–33]. The JLab 12 GeV beam upgrade was completed to allow the experimental access of the TCS production in the resonance free region. The large acceptance spectrometer CLAS12 started to taking data in 2018. And its the first TCS measurement on proton was recently published [30]. We have the selection of its results shown in Fig. 9. The photon circular polarization and forward-backward asymmetries were measured to be nonzero, providing strong evidence for the contribution of the quark-level mechanisms parameterized by GPDs to this reaction. The comparison of the measured polarization asymmetry with DVCS-data-constrained model predictions for the imaginary and real parts of GPD H points toward the interpretation of GPDs as universal functions. This is a great achievement, even with limited statistics. It is clear that more measurements are needed to expand the study of TCS.

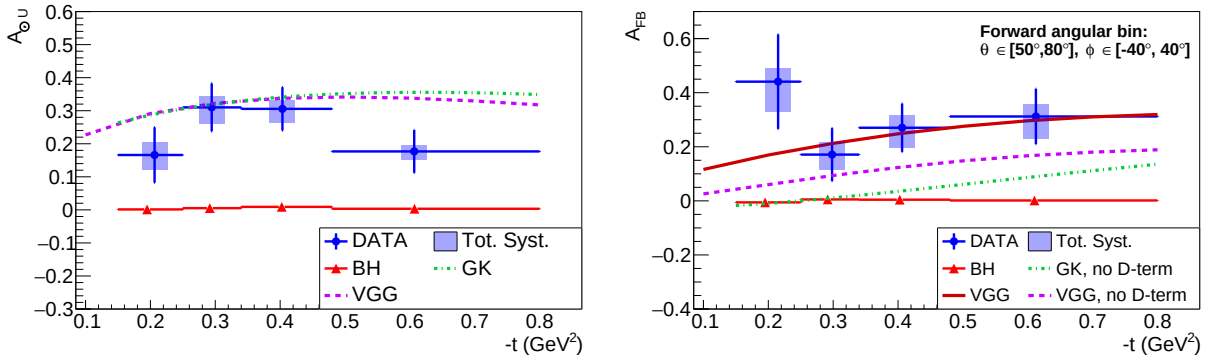

FIG. 9: The photon polarization asymmetry $A_{\odot U}$ (top) and forward-backward (bottom) asymmetries as a function of $-t$ at the averaged kinematic point $E_\gamma = 7.29 \pm 1.55$ GeV; $M = 1.80 \pm 0.26$ GeV. The errors on the averaged kinematic point are the standard deviations of the corresponding distributions of events. The data points are represented in blue with statistical vertical error bars. The horizontal bars represent the bin widths. The shaded error bars show the total systematic uncertainty. The red triangles show the asymmetry computed for simulated BH events. The dashed and dashed-dotted lines are the predictions of the VGG abd Gk models respectively. The solid line shows the model predictions of the VGG model with D-term. [30]

SoLID TCS experimental observables will include the same circularly polarized photon asymmetry and the forward-backward asymmetry just like CLAS12, but it can also study the unpolarized and beam polarized cross section with much more data. The kinematics can cover a wide range of squared four momentum transfer ($0.1 < -t < 1$ GeV^2), outgoing photon virtuality ($2.25 < Q'^2 < 9$ GeV^2) and skewness ($0.1 < \xi < 0.4$). SoLID TCS is the perfect next stage experiment after the CLAS12 TCS measurement. It will provide an essential cross-check by using a different large acceptance detector to measure the same process. This is a safe approach, since TCS is still a new tool for GPD studies. SoLID has excellent detection capability for e^+e^- leptons and protons. More importantly, it can handle high luminosity $10^{37}/\text{cm}^2/\text{s}$ which is 2 orders magnitude larger than CLAS12. Furthermore, the integrated luminosity of SoLID TCS 50e3 fb^{-1} is 250 times of the published CLAS12 data at 200 fb^{-1}. Even though SoLID acceptance of TCS events is about 1/4 of CLAS12, its full azimuthal coverage is ideal to control systematics. Overall, we expect a factor 60 increase of statistics, as shown in Fig. 10. This makes it possible to perform a mapping of TCS over the squared four momentum transfer, photon virtuality and skewness dependences at the same time. It will push the TCS study to a precision era, and together with DVCS, provide critical input to the global analyses to extract GPDs from high quality data. The comparative study of GPD H extracted from our measurement versus DVCS measurements at the same kinematic, will allow for a better understanding of factorization, Next leading order and higher twist effects in both TCS and DVCS [34], as their impacts are not the same on the Compton Form Factor values. It could potentially test the limits of GPD's universality, which would be a milestone in hadronic physics.

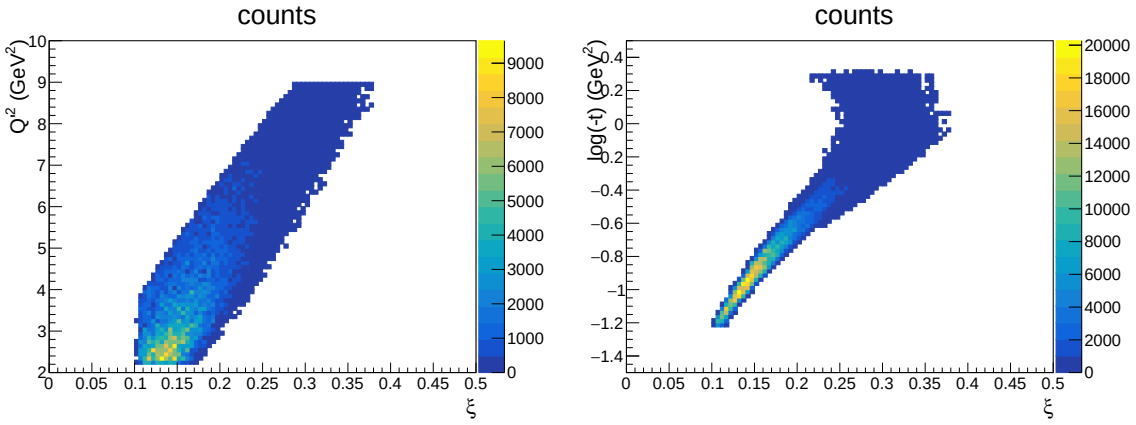

FIG. 10: The projected SoLID TCS statistics in the kinematic distribution of $Q'^2, \xi, log(-t)$

[1] A. Ali *et al.* (GlueX), First Measurement of Near-Threshold J/ψ Exclusive Photoproduction off the Proton, Phys. Rev. Lett. **123**, 072001 (2019), arXiv:1905.10811 [nucl-ex].

[2] B. Gittelman, K. Hanson, D. Larson, E. Loh, A. Silverman, *et al.*, Photoproduction of the psi (3100) Meson at 11-GeV, Phys.Rev.Lett. **35**, 1616 (1975).

[3] U. Camerini, J. Learned, R. Prepost, C. M. Spencer, D. Wiser, *et al.*, Photoproduction of the psi Particles, Phys.Rev.Lett. **35**, 483 (1975).

[4] R. Aaij *et al.* (LHCb), Observation of $J/\psi p$ Resonances Consistent with Pentaquark States in $\Lambda_b^0 \to J/\psi K^- p$ Decays, Phys. Rev. Lett. **115**, 072001 (2015), arXiv:1507.03414 [hep-ex].

[5] G. Baym, A. Aprahamian et al., An Assessment of U.S.-Based Electron-Ion Collider Science, Available at `https://www.nap.edu/read/25171` (2018).

[6] C. Alexandrou, S. Bacchio, M. Constantinou, J. Finkenrath, K. Hadjiyiannakou, K. Jansen, G. Koutsou, H. Panagopoulos, and G. Spanoudes, Complete flavor decomposition of the spin and momentum fraction of the proton using lattice QCD simulations at physical pion mass, Phys. Rev. D **101**, 094513 (2020), arXiv:2003.08486 [hep-lat].

[7] Y. Guo, X. Ji, and Y. Liu, QCD Analysis of Near-Threshold Photon-Proton Production of Heavy Quarkonium, Phys. Rev. D **103**, 096010 (2021), arXiv:2103.11506 [hep-ph].

[8] Y. Hatta and D.-L. Yang, Holographic J/ψ production near threshold and the proton mass problem, Phys. Rev. D **98**, 074003 (2018), arXiv:1808.02163 [hep-ph].

[9] Y. Hatta, A. Rajan, and K. Tanaka, Quark and gluon contributions to the QCD trace anomaly, JHEP **12**, 008, arXiv:1810.05116 [hep-ph].

[10] Y. Hatta, A. Rajan, and D.-L. Yang, Near threshold J/ψ and Υ photoproduction at JLab and RHIC, Phys. Rev. D **100**, 014032 (2019), arXiv:1906.00894 [hep-ph].

[11] F. He, P. Sun, and Y.-B. Yang (χQCD), Demonstration of the hadron mass origin from the QCD trace anomaly, Phys. Rev. D **104**, 074507 (2021), arXiv:2101.04942 [hep-lat].

[12] X. Ji, Y. Liu, and I. Zahed, Mass structure of hadrons and light-front sum rules in the $'t$ Hooft model, Phys. Rev. D **103**, 074002 (2021), arXiv:2010.06665 [hep-ph].

[13] X. Ji, Proton mass decomposition: naturalness and interpretations, Front. Phys. (Beijing) **16**, 64601 (2021), arXiv:2102.07830 [hep-ph].

[14] X. Ji and Y. Liu, Quantum anomalous energy effects on the nucleon mass, Sci. China Phys. Mech. Astron. **64**, 281012 (2021), arXiv:2101.04483 [hep-ph].

[15] D. E. Kharzeev, Mass radius of the proton, Phys. Rev. D **104**, 054015 (2021), arXiv:2102.00110 [hep-ph].

[16] K. A. Mamo and I. Zahed, Diffractive photoproduction of J/ψ and Υ using holographic QCD: gravitational form factors and GPD of gluons in the proton, Phys. Rev. D **101**, 086003 (2020), arXiv:1910.04707 [hep-ph].

[17] K. A. Mamo and I. Zahed, Nucleon mass radii and distribution: Holographic QCD, Lattice QCD and GlueX data, Phys. Rev. D **103**, 094010 (2021), arXiv:2103.03186 [hep-ph].

[18] D. A. Pefkou, D. C. Hackett, and P. E. Shanahan, Gluon gravitational structure of hadrons of different spin, Phys. Rev. D **105**, 054509 (2022), arXiv:2107.10368 [hep-lat].

[19] P. E. Shanahan and W. Detmold, Gluon gravitational form factors of the nucleon and the pion from lattice QCD, Phys. Rev. D **99**, 014511 (2019), arXiv:1810.04626 [hep-lat].

[20] P. Sun, X.-B. Tong, and F. Yuan, Perturbative QCD analysis of near threshold heavy quarkonium photoproduction at large momentum transfer, Phys. Lett. B **822**, 136655 (2021), arXiv:2103.12047 [hep-ph].

[21] Y.-B. Yang, J. Liang, Y.-J. Bi, Y. Chen, T. Draper, K.-F. Liu, and Z. Liu, Proton Mass Decomposition from the QCD Energy Momentum Tensor, Phys. Rev. Lett. **121**, 212001 (2018), arXiv:1808.08677 [hep-lat].

[22] R. Wang, J. Evslin, and X. Chen, The origin of proton mass from J/Ψ photo-production data, Eur. Phys. J. C **80**, 507 (2020), arXiv:1912.12040 [hep-ph].

[23] Solid (solenoidal large intensity device), updated preliminary conceptual design report, `https://solid.jlab.org/DocDB/0002/000282/001/solid-precdr-2019Nov.pdf` (2019).

[24] V. Sulkosky, L. Allison, C. Barber, T. Cao, Y. Ilieva, K. Jin, G. Kalicy, K. Park, N. Ton, and X. Zheng, Studies of relative gain and timing response of fine-mesh photomultiplier tubes in high magnetic fields, Nucl. Instrum. Meth. A **827**, 137 (2016), arXiv:1601.01903 [physics.ins-det].

[25] O. Gryniuk, S. Joosten, Z.-E. Meziani, and M. Vanderhaeghen, Υ photoproduction on the proton at the Electron-Ion Collider, Phys. Rev. D **102**, 014016 (Appendix A) (2020), arXiv:2005.09293 [hep-ph].

[26] S. Joosten, Argonne l/a-event generator, `https://eicweb.phy.anl.gov/monte_carlo/lager` (2021).

[27] Z. E. Meziani *et al.*, A Search for the LHCb Charmed 'Pentaquark' using Photo-Production of J/ψ at Threshold in Hall C at Jefferson Lab, (2016), arXiv:1609.00676 [hep-ex].

[28] R. Abdul Khalek *et al.*, Science Requirements and Detector Concepts for the Electron-Ion Collider: EIC Yellow Report, (2021), arXiv:2103.05419 [physics.ins-det].

[29] M. Boer, P. Nadel-Turonski, J. Zhang, Z. Zhao, *et al.*, Timelike compton scattering on the proton in e^+e^- pair production with solid at 11 gev, Jefferson Lab **E12-12-006A** (2015).

[30] P. Chatagnon, S. Niccolai, and S. *et al.*. Stepanyan (CLAS Collaboration), First measurement of timelike compton scattering, Phys. Rev. Lett. **127**, 262501 (2021).

[31] M. Boër, M. Guidal, and M. Vanderhaeghen, Timelike compton scattering off the proton and generalized parton distribu-

tions, Eur. Phys. J. A **51**, 103 (2015).
[32] M. Boër, M. Guidal, and M. Vanderhaeghen, Timelike compton scattering off the neutron and generalized parton distributions, Eur. Phys. J. A **52**, 33 (2016).
[33] Timelike compton scattering off a transversely polarized proton, JLab Hall C Proposal .
[34] M. Boër, Extraction of compton form factors with combined fits of spacelike and timelike deeply virtual compton scattering, JLab Hall C note (2019).